

RADIAL CORRELATIONS BETWEEN TWO QUARKS

UKQCD COLLABORATION

A.M. GREEN, J. KOPONEN, P. PENNANEN

Department of Physics and Helsinki Institute of Physics

P.O. Box 64, FIN-00014 University of Helsinki, Finland

E-mails: anthony.green@helsinki.fi, jmkopone@rock.helsinki.fi, petrus@hip.fi

C. MICHAEL

Department of Mathematical Sciences, University of Liverpool, L69 3BX, UK

E-mail: cmi@liv.ac.uk

In nuclear *many*-body problems the short-range correlation between two nucleons is well described by the corresponding correlation in the *two*-body problem. Therefore, as a first step in any attempt at an analogous description of *many-quark* systems, it is necessary to know the *two-quark* correlation. With this in mind, we study the light quark distribution in a heavy-light meson with a static heavy quark. The charge and matter radial distributions of these heavy-light mesons are measured on a lattice with a light quark mass about that of the strange quark. Both distributions can be well fitted upto $r \approx 0.7$ fm with the exponential form $w_i^2(r)$, where $w_i(r) = A \exp(-r/r_i)$. For the charge(c) and matter(m) distributions $r_c \approx 0.32(2)$ fm and $r_m \approx 0.24(2)$ fm. We also discuss the normalisation of the total charge (defined to be unity in the continuum limit) and matter integrated over all space, finding 1.30(5) and 0.4(1) respectively for a lattice spacing ≈ 0.17 fm.

1 Correlations between two nucleons

In nuclear many-body problems it is well known that the short-range correlations between pairs of nucleons are often well described by the corresponding correlations of the two-body problem. For example:

- **Few nucleon systems.** The NN correlations for the deuteron, ${}^3\text{He}$ and ${}^4\text{He}$, when normalised to each other at their maxima, are essentially indistinguishable upto about 2 fm. Only for larger internucleon distances do the binding energy differences play a role ¹.
- **Many-nucleon systems.** Often variational methods are used and a typical trial wavefunction is taken to be of the form

$$|\Psi_T\rangle = [\prod_{i<j} F_{ij}] |\Psi(\text{Shell Model})\rangle, \quad (1)$$

where $\Psi(\text{Shell Model})$ is simply a product(antisymmetrised) of single nucleon wavefunctions – encoding the long range correlations. However,

the short range physics between the NN pairs is in the

$$F_{ij} = \left[1 + \sum_m u_m(r_{ij}) O_{ij}^m \right], \quad (2)$$

where $O_{ij}^m = [1, \sigma_i \cdot \sigma_j, \dots] \otimes [1, \tau_i \cdot \tau_j]$ are the various spin and isospin operators for two nucleons. The variation then yields radial correlations $u_m(r_{ij})$ that are \approx 2-body problem correlations – see for example Ref. ².

- **Nuclear Matter** An extreme use in many-body systems of the two-body correlation is the Moszkowski-Scott separation method³ in nuclear matter. There the many-body wavefunction is taken to be of the form

$$\begin{aligned} \Psi(\text{Many} - \text{Body}) &= \Psi(\text{Two} - \text{Body}) \quad r < r_c \\ &= \sin(kr) \quad r \geq r_c, \end{aligned} \quad (3)$$

where r_c is the value of r at which $\Psi(\text{Two} - \text{Body})$ and $\sin(kr)$ and their derivatives equal each other.

The conclusion is that, in many-nucleon systems, the two-nucleon correlation from the two-body problem plays an important role.

The question can then be asked whether similar effects arise in multi-*quark* systems. This may help in the understanding of such systems. At present and in the foreseeable future, since lattice QCD calculations are restricted to very few quarks (upto four), some model *that encodes the results of these few-quark calculations* is needed in order to proceed to systems containing more quarks.

Earlier attempts by the present authors have concentrated on understanding the *energies* of four-quark systems in terms of interquark potentials. These involved four heavy quarks $(Q^2\bar{Q}^2)^4$ and the interaction of two heavy-light mesons $(Q^2\bar{q}^2)^5$. In neither case was it possible to understand the four-quark energies in terms of simply two-quark potentials – with the result indicating that a four-quark form-factor was necessary. This conclusion has also been supported by colour field measurements ⁶. Here, as a first step, the emphasis is on extracting the *radial correlation* between the two quarks of a heavy-light meson. Hopefully, this additional information on the $Q\bar{q}$ system will enable a less ambiguous model of this system to be made. At present, if through an operator $O(r)$, a transition between two two-quark states is calculated as $\langle \psi_1(r) | O(r) | \psi_2(r) \rangle$, then the ψ_i are first calculated as a byproduct of some differential equation containing some interquark potential - say $V(r) = a/r + br$. However, both the form of $V(r)$ and the equation into which it is inserted are not unique. The latter could range from a non-relativistic Schroedinger equation, if the quarks are heavy enough, through a series of equations that incorporate relativistic effects to varying degrees.

2 Heavy-light mesons ($Q\bar{q}$)

A study of heavy-light mesons is not just for the academic interest discussed above, since they are realised in nature. The best examples are the $B(5.28 \text{ GeV})$ and $B_s(5.37 \text{ GeV})$ mesons, which have quark structures $(\bar{b}u)$ and $(\bar{b}s)$. Since the b , s and u -quarks have masses of about 4.2, 0.1 and 0.001 GeV, we see that the B and B_s are indeed heavy-light mesons and can be thought of as the "Hydrogen atom" for quark systems. Currently the B -mesons are of particular interest, since they are expected to lead to a better understanding of CP violation and for this reason are being generated at so-called B -factories⁷.

More details of the following sections can be found in Ref.⁸.

2.1 Energies of Heavy-light mesons

The basic quantity for evaluating the energies of heavy-light mesons is the 2-point correlation function – see Fig. 1 a).

$$C(2, T) = \langle U^Q(\mathbf{x}, t, T) P(\mathbf{x}, t + T, t) \rangle, \quad (4)$$

where $U^Q(\mathbf{x}, t, T)$ is the heavy(infinite mass)-quark propagator and $P(\mathbf{x}, t + T, t)$ the light-quark propagator. The $\langle \dots \rangle$ means that $C(2)$ has been averaged over the whole lattice. Since the $C(2)$ decay as $\exp(-E_0 T)$, where E_0 is the energy of the ground state, we get

$$E_0 = -\ln \left[\frac{\langle C(2, T) \rangle}{\langle C(2, T-1) \rangle} \right] \quad \text{as } T \rightarrow \infty. \quad (5)$$

These energies were calculated in Ref.⁹ for the states

$$L_J = S_{1/2}, P_{1/2}, P_{3/2}, D_{3/2}, D_{5/2}, F$$

2.2 Heavy-Light radial correlations

Here the basic quantity is 3-point correlation function – see Fig. 1 b).

$$C(3, -t_2, t_1, \mathbf{r}) = \langle U^Q(\mathbf{x}, -t_2, t_1) P_1(\mathbf{x}, t_1; \mathbf{r}, 0) \Theta(\mathbf{r}) P_2(\mathbf{r}, 0; \mathbf{x}, -t_2) \rangle, \quad (6)$$

where the $P_{1,2}$ are the light anti-quark propagators that go from the Q at time t_1 to the point \mathbf{r} at $t = 0$ and then return to Q at time $-t_2$. The probe $\Theta(\mathbf{r})$ at \mathbf{r} is here considered to have two forms i) $\Theta = \gamma_4$ for measuring the charge distribution of the \bar{q} and ii) $\Theta = 1$ for measuring the matter distribution.

Knowing the $C(3)$ then the radial distributions are given by

$$F[C(\Theta, T, R)] = \frac{\langle C(3, \Theta, T, R) \rangle}{\langle C(2, T) \rangle}. \quad (7)$$

2.3 Lattice Parameters and Refinements

The essential lattice parameters are:

- 1) Lattice size $16^3 \times 24$
- 2) Quark-gluon coupling $\beta = 5.7$ giving a lattice spacing $\approx 0.17\text{fm}$
- 3) Light quark mass $\approx m_s$ – see Ref. ¹¹ as evidence for this.
- 4) Quenched Approximation i.e. quark-antiquark pairs are not included.

Eqs. 5 and 7 for the ground state energy(E_0) and correlations $F[C(\Theta, T, R)]$ are based on a single state constructed from the basic lattice. However, this can be extended by modifying this original lattice to give other states ($i, j, k...$). In this way the 2- and 3-point correlation functions can become matrices $C_{i,j}(2)$, $C_{i,j}(3, \mathbf{r})$. Their diagonalisation – by reducing the contamination of higher states on the ground state – then gives improved estimates of E_0 and $F[C(\Theta, T, R)]$. The mechanism for generating these addition states is fuzzing. This replaces a link on the lattice by a combination of neighbouring links to give a fuzzed link – with projection to SU3 implied – as

$$[\text{A fuzzed link}] = f_p \cdot [\text{Straight link}] + [\text{Sum of 4 spatial U-bends}].$$

This cycle can be repeat many times. Here, in addition to the basic state(L), two new states F1 and F2 are constructed using 2 and 6 cycles with $f_p = 2.5$. respectively.

3 Results

The lattice data $\langle C_{i,j}(2, T) \rangle$ and $\langle C_{i,j}(3, T, \mathbf{r}) \rangle$ can be analysed in several ways. Here two are presented: i) Visual and ii) Fitting with exponentials.

3.1 Visual

Fig. 2 shows from Eq. 7 the ratio $\langle C(3, R) \rangle / \langle C(2) \rangle$ for values of r upto 5 lattice spacings i.e. about 0.8fm. As $T \rightarrow \infty$, these clearly show plateaux, which give directly the desired charge or matter density.

3.2 Fitting with exponentials

A more precise method is to first fit the $\langle C_{i,j}(2, T) \rangle$ by the approximate expression

$$\tilde{C}_{ij}(2, T) = \sum_{\alpha=1}^3 v_i^\alpha \exp(-E_\alpha T) v_j^\alpha, \quad (8)$$

where the i, j refer to the states L, F1, F2. This results in the energy eigenvalues E_α and their eigenvectors v_i^α . These E_α are the energies quoted in Ref. ⁹. It

Table 1. The parametrization of the charge and matter densities as $w_m^2(r)$, where $w_m(r) = A_m \exp[-r/r_m]$.

	A_i	r_i (fm)	RMS Radius (fm)
Charge Density	0.26(1)	0.32(2)	0.55(3)
Matter Density	0.29(1)	0.24(2)	0.42(3)

is found that only data with $T \geq 4$ gives $\chi^2/dof \approx 1$. This means that 54 data points are fitted with 12 parameters.

Given the E_α and v_i^α the $C_{ij}(3, T, R)$ are then fitted by the approximate expression

$$\tilde{C}_{ij}(3, T, r) = \sum_{\alpha=1}^3 \sum_{\beta=1}^3 v_i^\alpha \exp[-E_\alpha t_1] x^{\alpha\beta}(r) \exp[-E_\beta t_2] v_j^\beta, \quad (9)$$

where the $x^{\alpha\beta}(r)$ are varied giving directly the desired charge or matter density. This needs $t_1 + t_2 \geq 8$ to get $\chi^2/dof \approx 1$ when fitting 18 data points with 3 parameters.

3.3 Analytic forms for the charge and matter densities

For the above charge ($i=c$) and matter ($i=m$) densities, it is of interest to express $x_i(r) = w_i^2(r)$ in the form $w_i(r) = A_i \exp(-r/r_i)$, where the parameters r_i and A_i are given for a global fit in Table 3.3. There, as in Fig. 3, it is clearly seen that the charge density has a significantly longer range than that of the matter density.

The fourier transforms of these densities lead to vector($i=v=c$) and scalar($i=s=m$) form factors that are usually expressed as $[F_{v,s}(q^2)] \propto (q^2 + M_{v,s}^2)^{-1}$. These are appropriate for the long-range part of $w_i^2(r)$ and lead to $M_v=0.9(1)$ and $M_s = 1.3(1)\text{GeV}$ and should be compared with the direct calculation of the $s\bar{s}$ vector and scalar mesons in Refs. ¹⁰ and ¹¹. The latter only involve 2-point correlation functions and so are more precise leading to $M_v=0.944(2)$ and $M_s = 1.61(6)\text{GeV}$.

3.4 Sum-rules

The above measures the densities at a few definite values of r . However, it is of interest to consider the sum-rules that sum over all values of r i.e.

$$F^{\text{sum}}[C(3)] = \frac{\langle \sum_{\mathbf{r}} C(3, \mathbf{r}) \rangle}{\langle C(2) \rangle}. \quad (10)$$

For the charge and matter densities this yields $I_c=1.30(5)$ and $I_m=0.4(1)$ respectively. On the other hand, integrating the above analytic expressions for $w_i(r)$ gives $1.5(1)$ and $0.7(1)$. These estimates are less reliable than the direct lattice sum, since much of the contributions are from small values of r where lattice artifacts enter.

By charge conservation we should get $I_c=1$ in the continuum limit – the quark charge having been defined as unity. However, it is known that renormalisation effects enter due to the finite lattice spacing. In Ref. ¹², for lattice parameters different to those used here, an overall renormalisation factor (F^V) of ≈ 0.8 is found for the vector(charge) vertex. Similar reductions are found in Ref. ¹³ for the axial vector operator. The inverse of our value of $I_c=1.30(5)$ could then be interpreted as a non-perturbative estimate of F^V as $0.77(3)$. In any case the conclusion is that our $I_c=1.30(5)$ is consistent with charge conservation for the continuum.

3.5 Dirac amplitude interpretation

In a relativistic quantum mechanical picture the above charge and matter distributions can be interpreted as $|g|^2 + |f|^2$ and $|g|^2 - |f|^2$, where g, f are the upper and lower components in the solution of the Dirac equation. Possibly this will now serve as a way to remove some of the ambiguities referred to at the end of Section 1 by ensuring that the solutions of the Dirac equation agree not only with the lattice or empirical energies but also the forms of $|g(r)|^2$ and $|f(r)|^2$.

Conclusions and Future

- The $S_{1/2}$ -wave charge and matter densities can be measured quite reliably out to $\approx 0.7\text{fm}$.
- Off-axis measurements can improve these results. In particular, it is interesting to see whether or not the charge density for $r = 5$ is indeed lower than the simple exponential drop off in Fig. 3. This would indicate that the confining potential is playing a role. Hopefully, the better statistics at the off-axis point $(3, 4)$ would clarify this point.
- The $P_{1/2}$, $P_{3/2}$, $D_{3/2}$, $D_{5/2}, \dots$ densities are now being measured.
- Understand the densities phenomenologically using the Dirac equation.
- Measure correlations in the $(Q^2 \bar{q}^2)$ system and check their form against the above $Q\bar{q}$ -correlations.

- Use larger β and lattices to get nearer the continuum limit.
- Replace the present quenched lattices by unquenched ones.
- Consider other operators, e.g. Pseudo-vector ($\gamma_\mu\gamma_5$) for $B^*B\pi$ coupling.

Acknowledgments

The authors wish to thank the Center for Scientific Computing in Espoo, Finland for making available resources without which this project could not have been carried out.

References

1. W. Glöckle and H. Kamada *Phys.Rev.Lett.* **71**, 971 (1993)
2. J. Carlson and R. Schiavilla , *Rev.Mod.Phys* **70**, 743 (1998)
3. S.A. Moszkowski and B.L. Scott, *Ann. of Phys* **36**, 2109 (1987).
4. P. Pennanen and A.M. Green , *Phys. Rev.* **57**, 3384 (1998).
5. A.M. Green, J. Koponen and P. Pennanen, *Phys. Rev. D* **61**, 014014 (2000).
6. P. Pennanen, A.M. Green and C. Michael *Phys. Rev. D* **59**, 014504 (1999).
7. H. Quinn and M. Witherell, *Sc.Am* **279**, 50 (1998)
8. A.M. Green, J. Koponen, P. Pennanen and C. Michael, "The Charge and Matter radial distributions of Heavy-Light mesons calculated on a lattice", hep-lat/0105027
9. C. Michael and J. Peisa, *Phys. Rev. D* **D58**, 034506 (1998) hep-lat/9802015
10. UKQCD Collaboration, C. McNeile and C. Michael, hep-lat/0010019
11. UKQCD Collaboration, H. Shanahan et al., *Phys. Rev. D* **D55**, 1548 (1997)
12. K.C. Bowler, L. Del Debbio, J.M. Flynn, G.N. Lacagnina, V.I. Lesk, C.M. Maynard and D.G. Richards, hep-lat/0007020
13. G.M. de Divitiis, L. Del Debbio, M. Di Pierro, J.M. Flynn, C. Michael and J. Peisa, JHEP 9810:010,1998 hep-lat/9807032

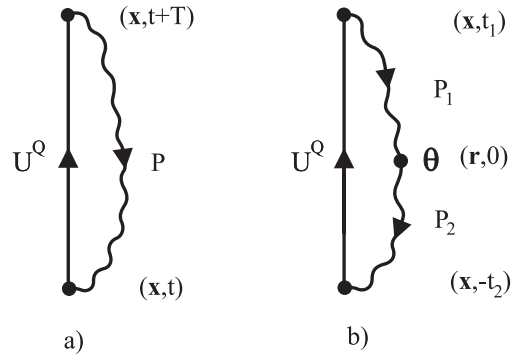


Figure 1. a) A two-point correlation function, b) A three-point correlation function.

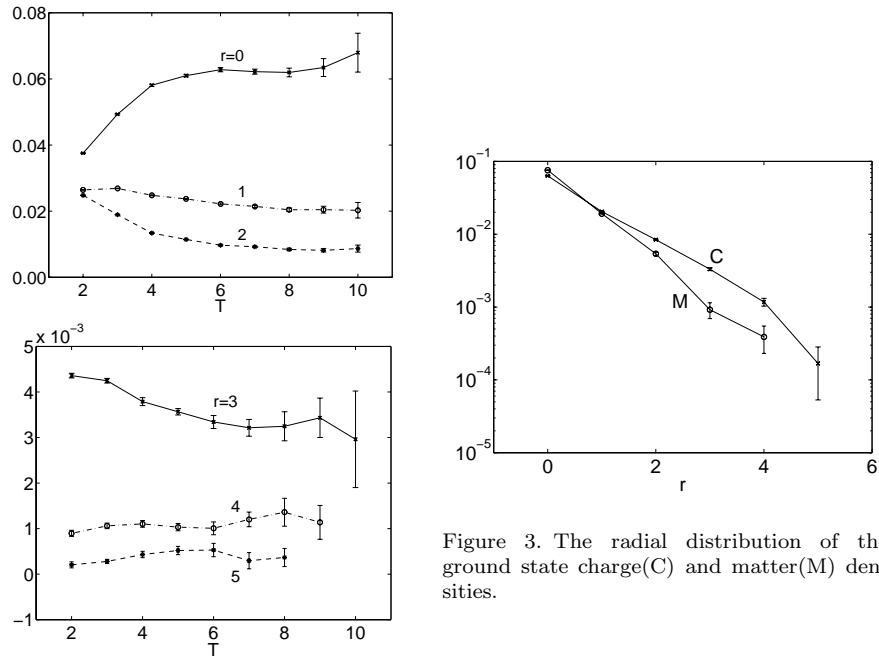


Figure 3. The radial distribution of the ground state charge(C) and matter(M) densities.

Figure 2. The ratio $\langle C(3, r) \rangle / \langle C(2) \rangle$ for $r = 0, \dots, 5$.

